Curing Mechanisms and Kinetic Analysis of DGEBA Cured with a Novel Imidazole Derivative Curing Agent Using DSC Techniques

Li Liu, Ming Li

Department of Polymer Science, School of Material Science and Engineering, Shanghai University, Jiading District, Shanghai 201800, People's Republic of China

ABSTRACT: A novel imidazole derivative, 2MI-*g*-CA, was obtained through the reaction of 2-methylimidazole (2MI) and cyanuric acid (CA) and characterized by means of elemental analysis, FTIR spectroscopy, ^{1}H NMR spectroscopy, and mass spectrometric analysis. The curing mechanisms and kinetics of diglycidyl ether of bisphenol A (DGEBA) using 2MI and 2MI-*g*-CA as curing agents were studied with differential scanning calorimetry (DSC) under dynamic and isothermal conditions. Both dynamic and isothermal DSC thermograms of DGEBA/2MI system showed two distinct exothermic peaks, whereas those of DGEBA/2MI-*g*-CA system showed only one distinct exothermic peak. These results indicated that the two systems have different initiation curing mechanisms. The apparent activation energies (E_a) obtained from DSC scanning runs using the Kissinger and Ozawa methods were 79.0, 83.0 kJ/mol and 84.2, 88.8 kJ/mol for DGEBA/2MI and DGEBA/2MI-*g*-CA systems, respectively. These values suggested the novel curing agent 2MI-*g*-CA exhibited greater levels of latency during cure or increased the pot life of epoxy resin system. In addition, under the same curing condition, the T_g values of DGEBA/2MI-*g*-CA system were about 25°C higher than those of DGEBA/2MI system, exhibiting a better thermal stability. © 2010 Wiley Periodicals, Inc. J Appl Polym Sci 117: 3220–3227, 2010

Key words: resins; DSC; activation energy; curing kinetics; imidazole derivative curing agent

INTRODUCTION

Epoxy resin is one of the most important thermosetting polymers, widely utilized in a number of industrial applications. Some of the uses of epoxy resins can be found in the adhesives, coatings, electronics, high-performance composite materials, and aerospace industries because of the excellent mechanical and chemical properties, such as high tensile and compressive strength, outstanding chemical resistance, high heat distortion temperature, low moisture adsorption, and so on.[1–6] In recent years, there has been a great increase in the number of applications of epoxy resins, especially in the electronics industry as encapsulating and packaging materials.[7–9] Curing of a resin system is the critical and productivity-controlling step in the fabrication of thermosetting-matrix composites.[1] Imidazoles are used as epoxy-curing agents owing to their fast catalytic action and also the fine mechanical properties, which they produce in the cured resin. Some imidazoles are high effective epoxy-curing agents and have superior physical properties (e.g., better heat resistance, lower tensile elongation, a higher modulus, and a wider range of cure temperature) than amine-cured system,[5] but unmodified imidazoles have low stability when mixed with epoxides (cure occurs slowly at room temperature) making them unsuitable for use in one-pot compositions, and therefore, much work has been carried out into stabilizing imidazoles for use as latent epoxy curing agents.[10,11]

In previous work on epoxy/imidazole systems, the mechanism of reaction between phenyl glycidyl ether (PGE) and 2-ethyl-4-methylimidazole (2, 4-EMI, which has both a secondary and a tertiary nitrogen) was widely investigated.[2,8,12,13] The curing mechanism which has been generally accepted was proposed by Barton and Shepherd.[10] The first step in the curing process for the PGE/2, 4-EMI system is the nucleophilic attack by the pyridine-type nitrogen (3-N) of the imidazole to open the epoxide ring. An OH adduct (1 : 1 adduct) is formed by the rearrangement of the zwitterion intermediate through a proton transfer. In the second step, the newly generated pyridine-type nitrogen attacks another epoxy group to produce the O^-/OH adduct (2 : 1 adduct). Evidence for this reaction mechanism was provided through the similar rates of adduct formation observed for both the 1 : 1 and 2 : 1 adducts, thus suggesting that both the adduct formation steps
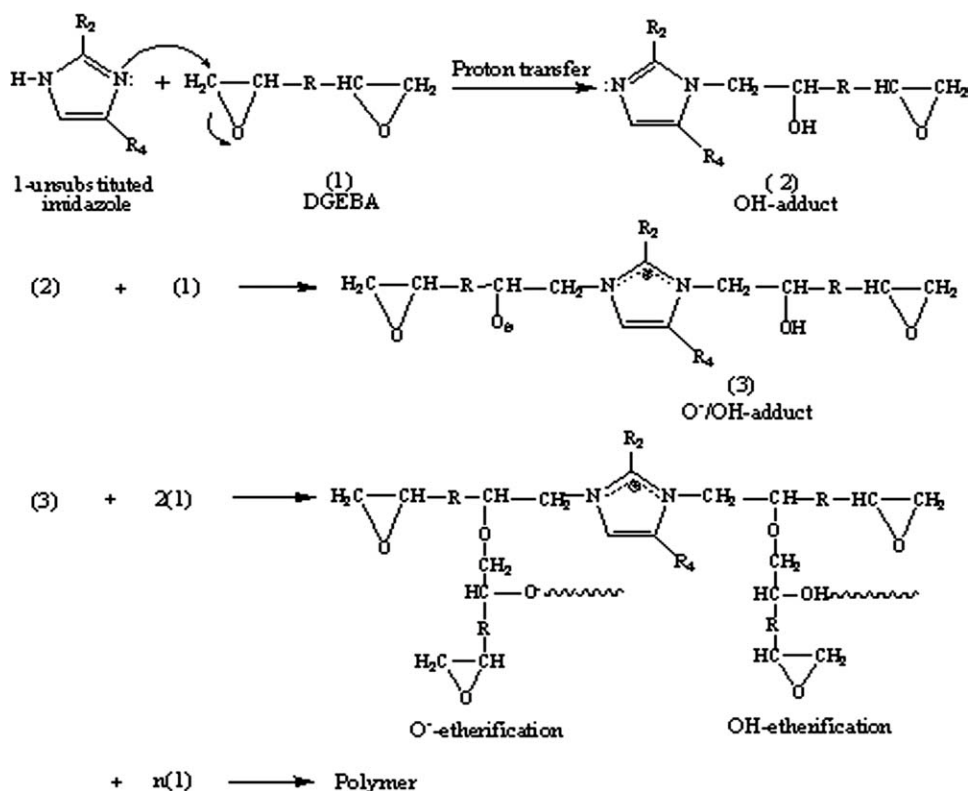
Figure 1 Proposed reaction mechanism for the curing of diepoxide with 1 unsubstitued imidazole.

involved the same type of amines (i.e., the more basic pyridine-type). The reaction of additional epoxide groups with the O⁻/OH adduct causes chain growth by two different etherification reactions: O⁻etherification and OH-etherification. These etherification reactions crosslink the resin and determine the final properties of the polymer network.[8] The proposed reaction mechanism for the DGEBA/imidazole system consists of two adduct reactions and two etherification reactions is shown in Figure 1.

Through the reaction mechanism proposed above, we can see that the pyridine-type nitrogen at 3-position of imidazole ring is the initial active site of the curing reaction.[4,6,10] In this work, we modified 2-methylimidazole (2MI) at 3-position by cyanuric acid (CA) and gained an imidazole-CA adduct, 2MI-*g*-CA. The curing behavior of neat diglycidyl ether of bisphenol A (DGEBA) using 2MI and 2MI-*g*-CA as curing agents were investigated by dynamic and iso-thermal differential scanning calorimetry (DSC). The kinetic parameters were compared to further eluci-date the polymerization mechanism and the curing characteristics of DGEBA/2MI-*g*-CA system.

EXPERIMENTAL

Materials

The structures of the materials used in this study are shown in Figure 2. Diglycidyl ether of bisphenol A

(DGEBA, type E-51, the epoxy equivalent was 185–196 g/eqiv) was obtained from Yueyang Petrochemi-cal Corporation, China. 2-Methylimidazole (2MI, 99%) was obtained from Shanghai Nuotai Chemical Co., China. Cyanuric acid (CA, 99%) was obtained from Shanghai Reagent, China. All chemicals were used as received without further purification.

Synthesis of 2MI-*g*-CA

The synthesis route to chemically modified 2MI with CA is shown in Figure 2. 2MI (8.21 g, 0.10 mol) dis-solved in 120 mL water was introduced into a flask equipped with a reflux condenser and a stir bar, and then introduced CA (12.91 g, 0.10 mol). The reaction mixture was boiled under agitation and nitrogen for 2 h. The reactants were completely dissolved in water, and then cooled the content. The product will precipitate from the solution slowly. After 12 h, the precipitated crystal was collected by filtration, and the final adduct 2MI-*g*-CA was dried in vacuum at 80°C for 24 h.

Characterization

Elemental analyses were performed with a Vario EL-III elemental analyzer. Fourier transform infrared (FTIR) spectra were recorded with a Nicolet Co., Ltd. 380 FTIR spectrometer (Thermo Fisher Scientific Co., Ltd.) by using KBr pellets. ^{1}H-NMR spectra
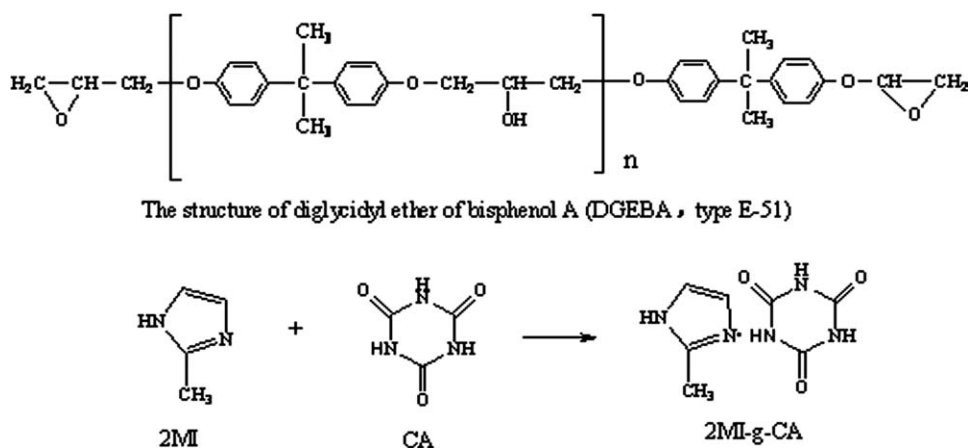
Figure 2 Structures of chemicals used and synthetic route.

were obtained using a BRUKER AV 500 spectrometer and mass spectrometric analyses were performed with Agilent 5975N GC-MS instrument (Agilent Technologies).

All DSC studies of the curing behavior were performed with the NETZSCH DSC 200 differential scanning calorimeter under a nitrogen atmosphere (30 cm^3/min). High purity indium and zinc were used to calibrate the calorimeter. All samples (8 ± 2 mg) were contained within sealed aluminum DSC pans.

Dynamic DSC measurements of the cure of DGEBA were performed from 40 to 300°C at five heating rates of 2, 5, 10, 15, and 20°C/min, using 2-MI and 2MI-g-CA as the curing agents at a concentration of 10 wt %. The samples which cured at 5°C/min were performed on a second scanning run at 5°C/min from 40 to 200°C to obtain their glass transition temperature (T_g) adopted the midpoint method provided by the NETZSCH DSC 200 analysis software.

Isothermal DSC studies were performed on DGEBA/2MI-g-CA system at 80, 100, 120°C and DGEBA/2MI at 80°C. A second scanning run at the heating rate of 5°C/min was performed from 40 to 300°C on all isothermally cured samples to obtain full cure. The final T_g was determined by a third scanning run at 5°C/min up to 200°C.

The degree of thermal cure was followed by monitoring the DSC heat flow as a result of the curing reactions. With the presumption that the heat flow as measured by DSC, dH/dt, is proportional to the rate of reaction da/dt, it is possible to determine the extent of fractional conversion, α, directly from the experimental curve by partial integration[1]:

$$\alpha = \frac{1}{\Delta H_{tot}} \int_0^t \frac{dH}{dt} dt \qquad (1)$$

The heat of reaction (ΔH) was obtained by integrating the DSC exothermic peak area of the heat-flow curve. In the dynamic DSC studies, ΔH obtained was assumed to represent the total heat of reaction (ΔH_{tot}) due to full cure, whereas in the isothermal DSC studies, a second residual scanning run was performed to achieve full cure. In the latter cases, ΔH_{tot} was obtained by the summation of the heat of reaction generated during the isothermal run (ΔH_{iso}) and the residual heat of reaction generated during the second scanning run (ΔH_{res}).[2] The activation energies (E_a) of the two systems were determined by both Kissinger method[14] and Ozawa method.[15,16]

RESULTS AND DISCUSSION

Synthesis of 2MI-g-CA

The addition reaction between the 2MI and CA can easily be carried out by heating both the reactants in the solvent under agitation. To verify the 2MI-g-CA synthesized in this work, the content of the element C, H, N in it were measured. The results are shown in Table I. It was found that the elemental analysis of the product prepared was basically in agreement with the calculated values.

FTIR spectrums of 2MI-g-CA are compared with its origins of 2MI and CA in Figure 3. The characteristic bands of both imidazole and cyanuricacid can be found in the 2MI-g-CA, including N—H stretching at 3470 cm^{-1}, N—H wagging vibration at 780 cm^{-1}, C—N stretching at 1110 cm^{-1}, C=N stretching at 1585 cm^{-1}, C=O stretching at 1720 cm^{-1}, C=C stretching at 1640 cm^{-1} and =CH rocking vibration at 1465 cm^{-1}.[6] Therefore, it is evidenced that the imidazole and CA in 2MI-g-CA keep original structure as desired. On the other hand, the most significant difference in the spectra lies in the flexure vibration absorption of C—H in imidazole ring at 2500–3200 cm^{-1} and imidazole ring vibration absorption at 1850 cm^{-1} disappears in the spectrum of 2MI-g-CA.

TABLE I
Elemental Analysis of 2MI-*g*-CA

Elements	C	H	N
Calculated value (%)	39.81	4.27	33.18
Analyzed value (%)	34.70	3.20	31.96

The result manifests that the hydrogen bond between 2MI and CA might have obstructed certain vibration modes.

^{1}H-NMR and Mass spectrum is further confirmed the chemical structure of 2MI-*g*-CA. ^{1}H-NMR spectrums of 2MI(CDCl$_3$, 500MHz) and 2MI-*g*-CA(DMSO-d$_6$, 500MHz) are shown in Figure 4. In the spectrum of 2MI: δ12.57(1H, NH); δ6.97(2H, =CH); δ2.43(3H, CH$_3$); in the spectrum of 2MI-*g*-CA: δ11.25(4H, 2MI+CA); δ6.84(2H, =CH); δ2.25(3H, CH$_3$). We can see the chemical shift in 2MI-*g*-CA is reduced comparing with 2MI, indicating CA have reacted with 2MI. MS m/e 206, 191, 189, 165, 149, 129(M+ of CA), 82(M+ of 2MI, 81, 55, 54.

Dynamic DSC analysis

Figure 5 shows typical DSC thermograms for the dynamic cure of epoxy resins with 10 wt % 2MI and 2MI-*g*-CA at five different heating rates of 2, 5, 10, 15, and 20°C/min, respectively. These thermograms provide information for the condition of cure reactions. Figure 5(a) shows that two distinct exothermic peaks are observed at all five different heating rates. Studies by Heise and Martin[8] and Ooi et al.[2] working with 1,3-unsubstituted imidazole (2,4-EMI and 2MI, respectively) have also observed a lower temperature peak (or shoulder). They attributed this lower temperature peak to the adduct formation in the first step as shown in Figure 1. The initiation of the etherification was marked by the appearance of the second exothermic peak during which ether
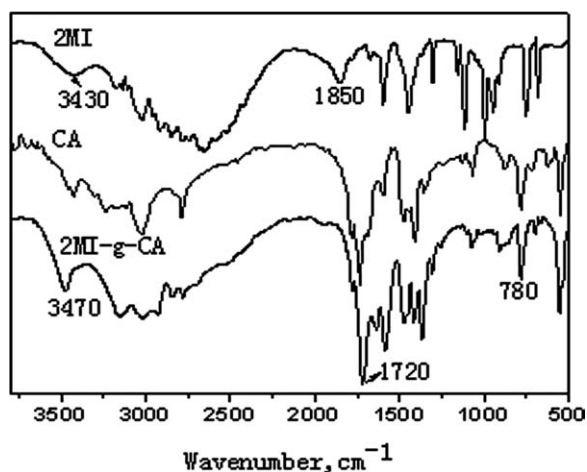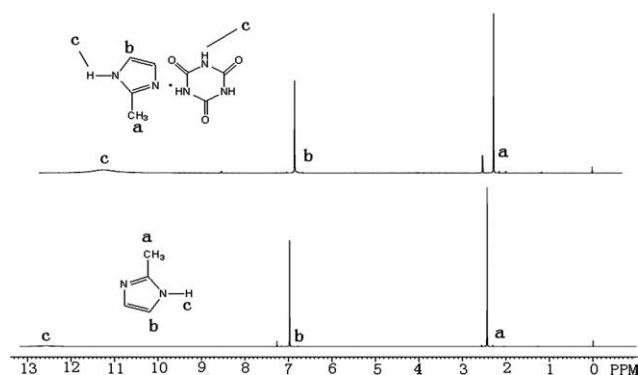

Figure 3 FTIR spectra of 2MI, CA, and 2MI-*g*-CA.

Figure 4 ^{1}H-NMR spectra of 2MI and 2MI-*g*-CA.

crosslinks were formed. On the contrary, only one distinct exothermic peak can be observed for the DGEBA/2MI-*g*-CA curing system in Figure 5(b). The results are evident that the curing mechanism using 2MI-*g*-CA as curing agent is different from that of using 2MI. The probable curing mechanism is that, as the temperature increasing, the hydrogen bond between 2MI and CA was destroyed and 2MI-*g*-CA complexes was dissociated into CA and 2MI at a relative high temperature (about 110°C), and then the released 2MI cured DGEBA following the steps as shown in Figure 1. Because the temperature was high, the exothermic peak of the adduct formation merged into the one of the etherification reaction, there was only one exothermic peak in the thermograms of DGEBA/2MI-*g*-CA system. The probable mechanism of curing reaction between DGEBA and the complex 2MI-*g*-CA is shown in Figure 6. In addition, it is interesting to note that for the DGEBA/2MI-*g*-CA curing system shown in Figure 5(b), a high temperature exothermic peak can also be observed at about 220°C, which is noticeable at heating rate of 10, 15, and 20°C/min. There may be two causes for the result. One may be associated with imidazole regeneration by *N*-dealkylation and/or β-elimination which are well expatiated by Ooi et al.[2] The generation of the original imidazole by *N*-dealkylation and/or β-elimination may then initiate further polymerization. The other may attribute to 2MI-*g*-CA containing the carbonyl groups which are able to participate in the polymerization as a hardener agent (like to acid anhydrides) to increase the crosslinking density at a relatively higher temperature according the result reported by Fung Fuh Wong.[5]

From the curves in Figure 5, we can also observe that the exothermic peak shifts to a higher temperature with higher heating rate. Information about the nature of the curing reaction such as initial curing temperature (T_i), maximum exothermic peak temperature (T_p), final cure temperature (T_f), and enthalpy of cure reaction (ΔH) at different scan rates of the two curing systems are summarized in Table II and
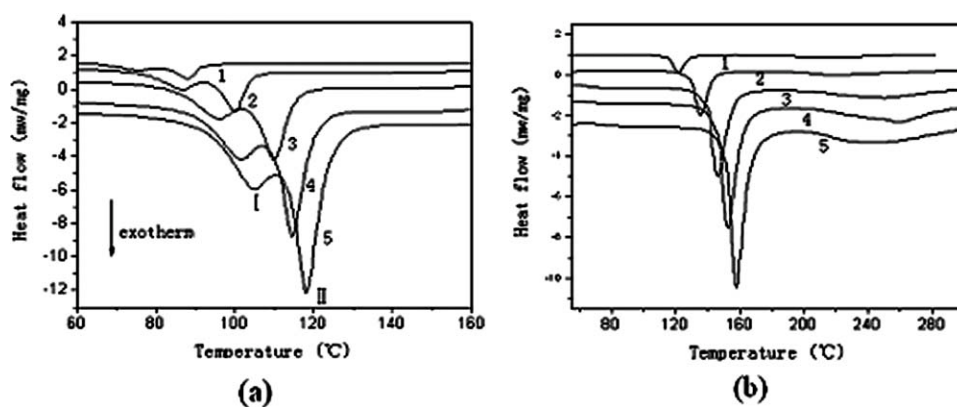
Figure 5 Typical dynamic DSC curves recorded for the two systems at different heating rates: (1) 2; (2) 5; (3) 10; (4) 15; (5) 20°C/min. (a) DGEBA/2MI and (b) DGEBA/2MI-*g*-CA.
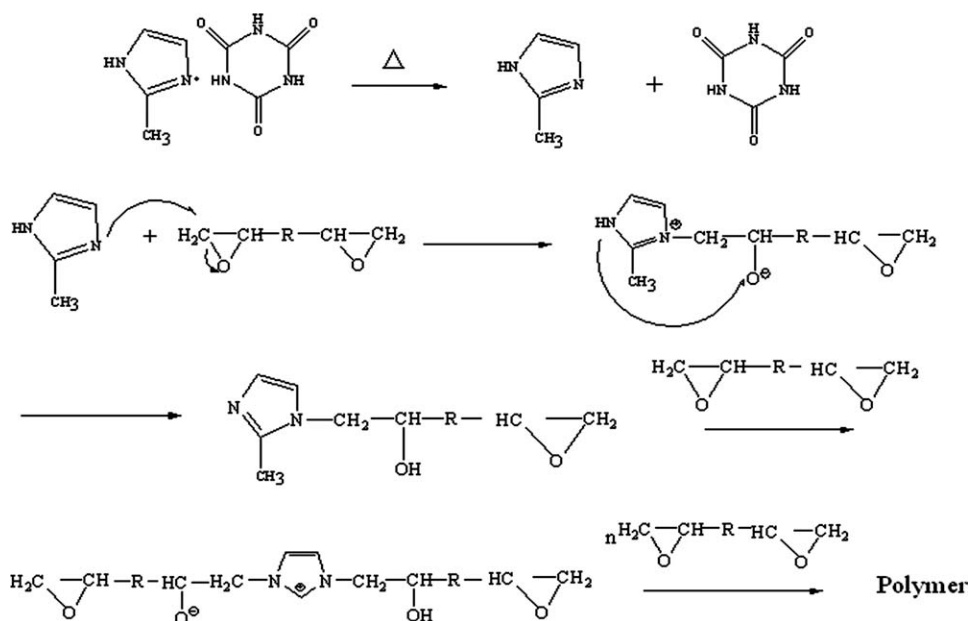

Figure 6 Mechanism of curing reaction between DGEBA and 2MI-*g*-CA.

TABLE II
Data from the Analysis of Dynamic DSC Measurements

Curing agent	Heating rate (°C/min)	T_i (°C)	T_p (°C)	T_f (°C)	ΔH (J/g)	E_a (KJ/mol)
2MI	2	66	75	92	304	E_aK 79.0
	5	76	86	104	367	E_aO 83.0
	10	84	96	115	372	
	15	90	101	120	398	
	20	93	105	124	422	
2MI-*g*-CA	2	115	122	129	377	E_aK 84.2
	5	129	136	143	382	E_aO 88.8
	10	140	146	156	416	
	15	146	153	162	427	
	20	152	158	167	368	

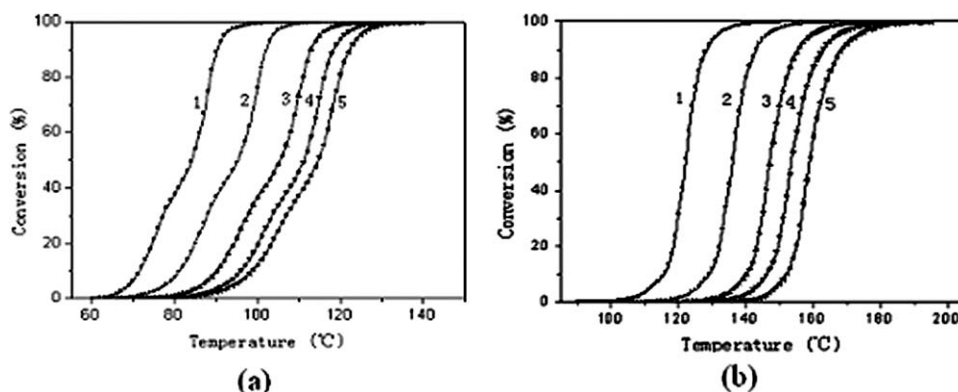E_aK, Kissinger method; E_aO, Ozawa method.

Figure 7 Fractional conversion as a function of temperatures for the two systems: (1) 2; (2) 5; (3) 10; (4) 15; (5) 20°C/min. (a) DGEBA/2MI and (b) DGEBA/2MI-*g*-CA.

fractional conversions as a function of temperature for the two curing systems estimated from the DSC thermograms are shown in Figure 7.

From Table II, it is clear that the cure reaction of the DGEBA/2MI system is carried out at relative low temperature, but in the DGEBA/2MI-*g*-CA system, the T_i, T_p, and T_f are 50°C higher than the temperature of DGEBA/2MI system at the same heating rate, respectively. From Figure 7, we can see that at the same conversion, the temperature of DGEBA/2MI-*g*-CA are also about 50°C higher than DGEBA/2MI system. All of these mean that 2MI-*g*-CA has improved storage stability than unmodified 2MI.

Kissinger method[14] and Ozawa method[15,16] were adopted to calculate the activation energies (E_a) for DGEBA cured with 2MI and 2MI-*g*-CA. According to Kissinger method, the E_a can be determined using the following equations:

$$\ln\left[\frac{\beta}{T_p^2}\right] = \frac{-E_a}{RT_p} + \ln\left[\frac{AR}{E_a}\right] \tag{2}$$

where β is the heating rate; T_p is the temperature of the maximum exothermic peak; A is the pre-expo-
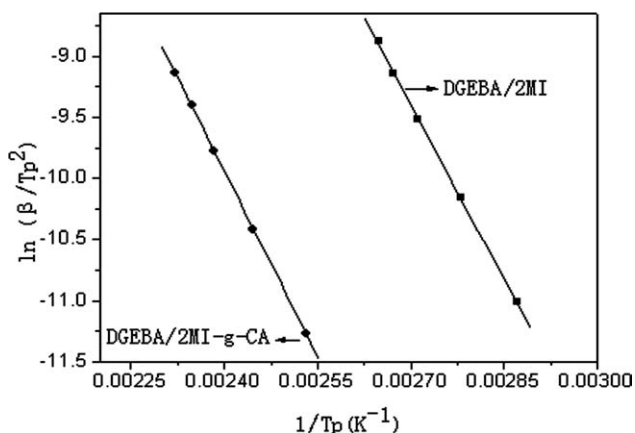
nential factor; and R is the gas constant (8.314 J/g mole K). By plotting $1/T_p$ versus $\ln\beta/T_p^2$ at different heating rates, values of E_a can be obtained from the slope of the straight lines (shown in Fig. 8). The activation energies determined for the curing reaction of DGEBA/2MI and DGEBA/2MI-*g*-CA are 79.0 and 84.22 kJ/mol, respectively.

According to Ozawa method, the relationship between the E_a, heating rate (β), and peak exothermic temperature (T_p) can be described as follows:

$$E_a = \frac{-R}{1.025} \times \frac{\Delta\ln\beta}{\Delta 1/T_p} \tag{3}$$

By plotting $1/T_p$ versus $\ln\beta$ at different heating rates, the values of E_a were obtained from the slope of the straight lines (shown in Fig. 9). The activation energies determined for the curing reaction of DGEBA/2MI and DGEBA/2MI-*g*-CA are 83.0 and 88.8 kJ/mol, respectively. The activation energies of DGEBA/2MI-*g*-CA determined by both two methods are bigger than that of DGEBA/2MI. The results
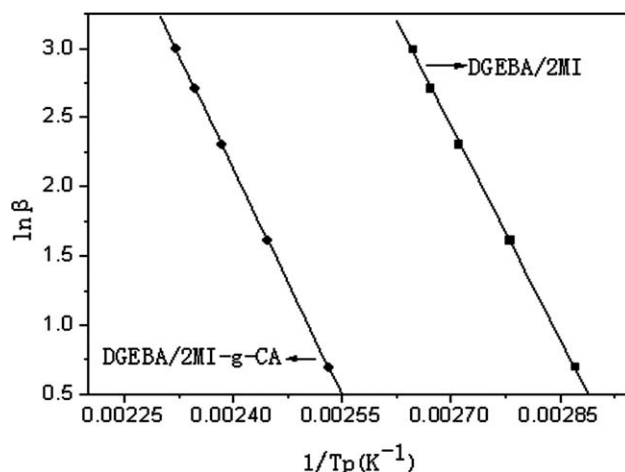

Figure 8 Kissinger method plot for apparent activation energy determination of the two curing systems.

Figure 9 Ozawo method plot for apparent activation energy determination of the two curing systems.
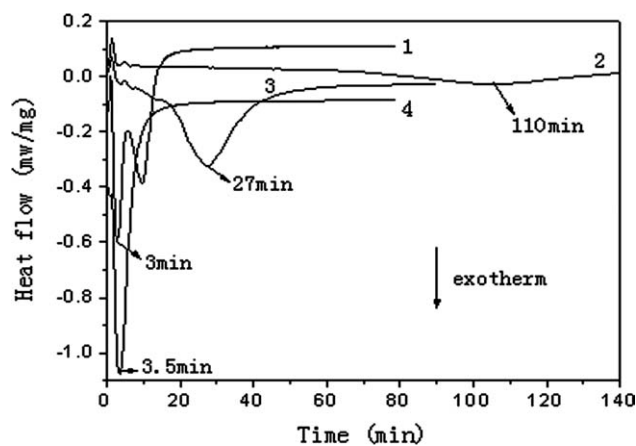
Figure 10 Isothermal DSC scans of two curing systems at different temperatures: (1) DGEBA/2MI system cured at 80°C and (2), (3), (4) DGEBA/2MI-g-CA system cured at 80, 100, 120°C, respectively.

indicate that the novel curing agent 2MI-g-CA exhibited greater levels of latency during cure or increased the pot life of epoxy resin system on curing kinetics.

Isothermal DSC analysis

Typical DSC isothermal thermograms for DGEBA cured by 2MI and 2MI-g-CA are shown in Figure 10. The analyses of the data are given in Table III. There are two distinct exothermic peaks for DGEBA/2MI system cured at 80°C, whereas only one peak for DGEBA/2MI-g-CA system cured at 80, 100, and 120°C. This is well documented the mechanism proposed above. From Figure 10, we can see that in the DGEBA/2MI system, the first exothermic peak appears at 3 min, the second appears at 10 min, and at about 20 min the curing process is over ultimately (the curve 1). These results indicate 2MI is a high effective epoxy resin hardener at 80°C. In the DGEBA/2MI-g-CA system cured at 80°C, there is no detectable exothermic peak within 60 min, implying nearly no curing reaction takes place. It does not appear a dispersion exothermic peak until at 110 min. It is evident that 2MI-g-CA takes on good thermal latency in epoxy resin at 80°C. When the curing temperature is up to 120°C, DGEBA/2MI-g-CA system has an exothermic peak at 3.5 min and the cur-

ing process is finished within 10 min, indicating 2MI-g-CA is a high effective epoxy resin hardener at 120°C. In a word, 2MI-g-CA system takes on a better storage stability at relative low temperature, but when the temperature is higher 2MI-g-CA can also cure the epoxy resin effectively at a short time. Therefore, 2MI-g-CA can be used as latent epoxy-curing agents at certain condition.

The measurement of glass transition temperature (T_g)

The glass transition temperature (T_g) is a second-order thermodynamic response and it involves a temperature zone within which long-range molecular motion and greater rotational freedom occur.[10] The factors which determine the glass transition temperature (T_g) are many and complicated, such as the structure, nature, and the concentration of the curing agent. In addition, Barton et al.[10] reported that different curing schedules also resulted in different T_g's and the final T_g's from isothermal curing processes are higher than those from dynamic curing processes. In this work, it was obtained as the intercept of the two tangents of the heat-flow temperature curve before and during the transition temperature. This T_g determination was adopted the midpoint method provided by the NETZSCH DSC 200 analysis software. The glass transition temperature (T_g) of DGEBA/2MI and DGEBA/2MI-g-CA samples are shown in Figure 11. We can see the final T_g's from isothermal curing (107, 134°C) are higher than those from dynamic curing (104, 127°C), comparing well with the disciplinarian reported by Barton et al. What's more, under the same curing condition, the T_g values of DGEBA/2MI-g-CA system are about 25°C higher than that of DGEBA/2MI system. The results indicate that DGEBA/2MI-g-CA system has a better thermal stability.

CONCLUSIONS

A novel imidazole derivative, 2MI-g-CA, was successfully synthesized by the reaction of 2MI and CA. Both dynamic and isothermal DSC thermograms of DGEBA/2MI system showed two distinct exothermic peaks. The first peak (shoulder) was assigned to the adduct formation, whereas the second (major)

TABLE III
Data from the Analysis of Isothermal DSC Measurements

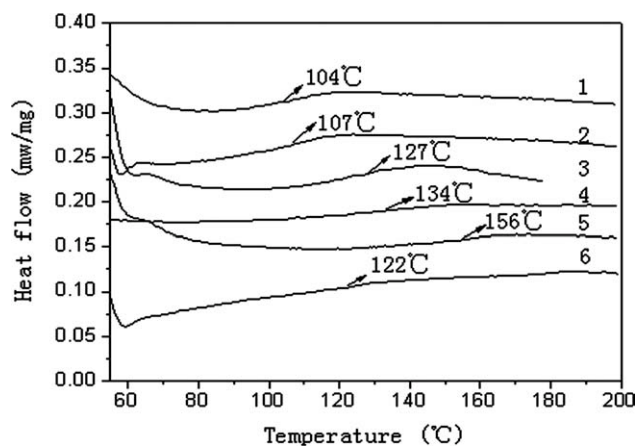| Cruing agent	Temperature (°C)	T_{max} (min)	ΔH_{iso} (J/g)	ΔH_{res} (J/g)	ΔH_{tot} (J/g)
2MI	80	3	240	73	313
2MI-g-CA	80	110	98	90	188
	100	27	215	60	275
	120	3.5	172	7	179

Figure 11 Glass transition region from DSC: (1) DGEBA/2MI sample dynamic cured at 5°C/min; (2) DGEBA/2MI sample isothermal cured at 80°C; (3) DGEBA/2MI-*g*-CA sample dynamic cured at 5°C/min; and (4), (5), (6) DGEBA/2MI-*g*-CA sample isothermal cured at 80, 100, 120°C, respectively.

peak was due to the etherification reaction. On the contrary, those of DGEBA/2MI-*g*-CA system showed only one exothermic peak, indicating that the two systems have different initiation mechanisms. The cause resulting in the different mechanism of DGEBA/2MI-*g*-CA system is that the hydrogen bond between 2MI and CA in 2MI-*g*-CA protects 2MI from occurring curing reaction at room temperature, when the temperature is up to about 110°C, the hydrogen bond between them will be destroyed and 2MI-*g*-CA will be dissociated into 2MI and CA, then the released 2MI can initiate the curing reaction. Both dynamic and isothermal DSC thermograms showed that DGEBA/2MI-*g*-CA system cured at a relatively higher temperature than DGEBA/2MI system, also higher than the DGEBA/EMI-*g*-BGE system which is reported by Wang Fang.[1] The results suggest the novel curing agent 2MI-*g*-CA exhibited greater levels of latency during cure or increased the pot life of epoxy resin system. The valves of the apparent activation energy E_a indicated the conclusion further on curing kinetics. Finally, DGEBA/2MI-*g*-CA system exhibited a better thermal stability through the analyses of the T_g values. The other mechanical properties will be investigated later.

References

1. Fang, W.; Jun, X.; Jing-Wen, W.; Shu-Qin, L. J Appl Polym Sci 2008, 107, 223.
2. Ooi, S. K.; Cook, W. D.; Simon, G. P.; Such, C. H. Polymer 2000, 41, 3639.
3. Park, S.-J.; Jin, F.-L. Polym Degrad Stab 2004, 86, 515.
4. Abdollah, O.; Leonardo, C. S.; Abbas, A. R.; Mousa, G. Thermochim Acta 2008, 468, 39.
5. Fuh Wong, F.; Chen, K.-L.; Lin, C. M.; Yeh, M.-Y. J Appl Polym Sci 2007, 104, 3292.
6. Yin, T.; Rong, M. Z.; Zhang, M. Q.; Yang, G. C. Compos Sci Technol 2007, 67, 201.
7. Chen, Y.-C.; Chiu, W.-Y.; Lin, K.-F. J Polym Sci Part A: Polym Chem 1999, 37, 3233.
8. Heise, M. S.; Martin, G. C. Macromolecules 1989, 22, 99.
9. Ghaemy, M.; Sdjady, S. J Appl Polym Sci 2006, 100, 2634.
10. Barton, J. M.; Hamerton, I.; Howlin, B. J.; Jones, J. R.; Liu, S. Polymer 1998, 10, 1929.
11. Abdollah, O.; Leonardo, C. S.; Abbas, A. R.; Mousa, G. Eur Polym J 2008, 44, 769.
12. Barton, J. M.; Shepherd, P. M. Makromol Chem 1975, 176, 919.
13. Barton, J. M.; Buist, G. J.; Hamerton, I.; Howlin, B. J.; Jones, J. R.; Liu, S. J Mater Chem 1994, 4, 379.
14. Kissinger, H. E. Anal Chem 1957, 29, 1702.
15. Ozawa, T. Bull Chem Soc Jpn 1965, 38, 1881.
16. Ozawa, T. J Therm Anal 1970, 2, 301.